Cenozoic contourites in the eastern Great Australian Bight, offshore southern Australia: implications for the onset of the Leeuwin Current

Christopher A-L. Jackson*
Craig Magee
Esther R. Hunt-Stewart

Basins Research Group (BRG), Department of Earth Science & Engineering, Imperial College, Prince Consort Road, LONDON, SW7 2BP, UK

**corresponding author email: c.jackson@imperial.ac.uk*

ABSTRACT

Thermohaline oceanic currents influence global heat transfer, controlling local and global variations in climate, biodiversity, and the terrestrial biosphere. Paleoceanographic studies typically use biostratigraphic and geochemical proxies to reconstruct the dynamics of these currents in Earth's ancient oceans, although seismic reflection data have also been successfully employed, most commonly in the North Atlantic Ocean. Here we use 2D seismic reflection data from the Ceduna Sub-basin, Great Australian Bight, offshore southern Australia to describe middle Eocene-to-Recent contourites deposited within an overall carbonate-dominated succession. These deposits comprise large (100 m wavelength by up to 50 m tall) bedforms and deep (10–90 m), wide (up to 3 km) erosional scours. The scours are particularly well-developed at one specific stratigraphic level, defining moats that encircle Middle Eocene shield volcanoes, which formed syn-depositional bathymetric highs. We suggest that sediment erosion, transport, and deposition record middle Eocene initiation of the Leeuwin Current, one of the most important ocean currents in the southern hemisphere. Deepest seabed scouring occurs within the middle of the middle Eocene-to-Recent sequence, and may reflect middle Miocene waxing of the so-called 'proto-Leeuwin Current', possibly driven by changes in ocean circulation patterns caused by the Miocene Global Optimum. The results of this seismic reflection-based study are consistent with results derived from other paleoceanographic proxies, thereby highlighting the continued key role seismic reflection data have in understanding the occurrence, geographical distribution, and significance of ancient ocean currents.

Introduction. By influencing seawater temperature and salinity, ocean current activity controls regional and global trends in climate and biodiversity. Determining past changes in thermohaline circulation patterns in the world's oceans is thus important to understanding how climate and biodiversity varied in deep time and, therefore, may change in the future (cf. "geological analogues" of IPCC, 2007; see also e.g., Henderson, 2002; Wunsch, 2002; Rahmstorf, 2003; Wyrwoll et al., 2009). Paleooceanographic analysis commonly relies on biostratigraphic and geochemical proxy data, which: (i) are expensive to collect, and typically only collected on academic scientific cruises (e.g. IODP); (ii) are spatially limited (i.e. collected over a relatively small area within a discrete stratigraphic intervals); and (iii) do not typically provide a physical (i.e. stratigraphic) record of the initiation, extent, and decay of oceanographic currents (e.g. von Blackenburg, 1999; Henderson, 2002). Seismic reflection data can image very large (up to 10's of metre thick, and several hundred-to-tens of kilometres long) contourite systems, which provide an explicit record of ocean current-driven, erosion and reworking of the ancient seabed (e.g. Boldreel et al., 1998; Davies et al., 2001; Faugères et al., 1999; Rebesco and Stow, 2001; Stow et al., 2003; Due et al., 2006; Hohbein et al., 2012; Rebesco et al., 2014). When integrated with more widely used paleoceanographic proxies, as they have been most commonly and successfully in the North Atlantic Ocean (e.g. Tucholke, 1979; Tucholke & Mountain, 1979; Mountain & Miller, 1992; Davies et al., 2001; Müller-Michaelis et al., 2013; Calvin Campbell & Mosher, 2016; Boyle et al., 2017), seismic reflection data form a key part of the oceanographer's toolkit.

In this study we use 2D seismic reflection data from the Ceduna Sub-basin, Great Australian Bight, offshore southern Australia to identify and map middle Eocene-to-Recent contourites, which possibly record the middle Eocene initiation of the current now known as the Leeuwin Current. Although its age of initiation is debated, the present Leeuwin Current is the longest (5000 km) and one of the most important ocean currents in the southern hemisphere (Fig. 1A). It is connected to and samples the global thermohaline system via the Indonesian Gateway (Feng et al., 2009), flowing southwards at relatively shallow depths (<300 m) and modest speeds (<2 m s^{-1}, but as low as 0.3–0.5 m s^{-1} in the Great Australian Bight) along the western coast of Australia and thereafter eastwards into the Great Australian Bight (Fig. 1A) (Cresswell and Golding, 1980; Cresswell & Domingues, 2009). Transporting warm, low-salinity waters derived from the South Equatorial Current within a relatively narrow band (<100 km), the Leeuwin Current contributes to climatic variations and vegetation patterns (e.g., Caputi, 2001; Feng et al., 2009; Wyrwoll et al., 2009), and continent-scale biodiversity patterns by transporting otherwise low-latitude fauna to anomalously high latitudes (e.g., Cann and Clarke, 1993; McGowran et al., 1997; Passlow et al., 1997). By providing what we think is the first physical evidence for ocean current activity in relatively deepwater, offshore southern Australia, our seismic reflection-based study broadly supports studies proposing a middle Eocene initiation age for the Leeuwin Current (McGowran et al., 1997; see also Feary and James, 1995, 1998). More generically, our study confirms that seismic reflection data, if integrated with biostratigraphic and geochemical proxies, can help improve our understanding of deep-time dynamics of the Earth's ancient oceans.

Geological Setting. The Ceduna Sub-basin is located in the Bight Basin, offshore southern Australia (Fig. 1A), and formed in response to Jurassic-to-Early Cretaceous rifting and Early Cretaceous-to-Recent, post-rift thermal subsidence. Numerous submarine volcanoes were emplaced during earliest Middle Eocene magmatism at *ca*. 42 Ma (the 'Bight Basin Igneous Complex'; Schofield & Totterdell, 2008; Jackson, 2012; Magee et al., 2013), with the volcanoes onlapped by the fully marine, middle Eocene-to-Recent, carbonate-dominated Nullarbor Limestone (Fig. 1B) (Schofield & Totterdell, 2008). Schofield & Totterdell (2008) and Jackson (2012) identify numerous scours in the Nullarbor Limestone, although they do not explore their age or origin, their genetic relationship to the middle Eocene volcanoes, or the potential paleoceanographic significance of their causal current. There are no direct constraints on middle Eocene-to-Recent water depths in the distal Ceduna Sub-basin, although the heights of Eocene clinoforms along the northern basin margin (Feary and James, 1995, 1998; McGowran et al., 1997) and the preservation of pristine submarine volcanoes within fully marine sediments (Magee et al., 2013; Jackson (2012) suggests the basin deepened to a few hundred metres (i.e. broadly comparable to the present depth of the Leeuwin Current; see above) during middle Eocene flooding (see also McGowran et al., 1997; Shafik, 1983; 1990). The Ceduna Sub-basin lies outboard of the modern day shelf edge in water depths of 200–4000 m; the seabed in the study area is below the influence of the modern Leeuwin Current, which extends to depths of *c*. 300 m (Feng et al., 2009).

Paleoceanography of the Great Australian Bight. The Quaternary extent and dynamics of the Leeuwin Current in the Great Australian Bight are relatively well understood (Cresswell and Golding, 1980; Feng et al., 2009; Wyrwoll et al., 2009), whereas its timing of initiation, and its pre-Quaternary eastward 'reach' into the Great Australian Bight, remain uncertain.

Based on their discovery of warm-water, Eocene microfauna in the Otway Basin, McGowran et al. (1997) suggested an even older, middle Eocene age of initiation for the Leeuwin Current in the Great Australian Bight, arguing these fauna were likely derived from warm low-latitudes (i.e. via the proto-Leeuwin Current) and not cold high-latitudes (i.e. via the Flinders Current) (Fig. 1A); this interpretation is supported by fully coupled climate model simulations (Huber et al., 2004). However, pre-Early Oligocene initiation of the Leeuwin Current is disputed given that opening of the Tasmanian Gateway, which facilitated eastwards flow of warm ocean waters along southern Australia into the Pacific, did not occur until the Early Oligocene (e.g. Stickley et al., 2004; Wyrwoll et al., 2009). These studies together suggest the proto-Leeuwin Current in some way shaped the Eocene-to-Recent stratigraphic evolution of the Great Australian Bight shelfal regions, although the stratigraphic expression of time-equivalent, basin-centre units, which should also record the initiation and influence of this important ocean current, has yet to be documented.

Although middle Eocene initiation of the Leeuwin Current is disputed, there is evidence from IODP Leg 182 that anomalously warm waters entered the Great Australian Bight during at least the middle Miocene, possibly in response changes in ocean circulation driven by the Miocene Climatic Optimum (e.g. Savin et al., 1975; Feary and James, 1995, 1998; Gourley and Gallagher, 2004). For example, McGowran et al. (1997) document the 'Little Barrier Reef', a thick (350 m), laterally extensive (>475 km long), rimmed carbonate platform developed along the northern margin of the Bight Basin (Fig. 1A).

Data and methods. Our dataset consists of 109 time-migrated, zero-phase, 2D seismic reflection lines that have a cumulative line length of *c*. 13,000 km and cover *c*. 44,000 km^2 of the central Ceduna Sub-basin (Fig. 1A). The NW- and NE-trending lines are spaced 4–16 km and 4–8 km, respectively (Fig. 2).

Biostratigraphic data from the Potoroo-1 borehole, which is located c. 200 km NW of the main study area, directly constrain: (i) the age of a key, regionally mappable seismic horizon defining the top of the Cretaceous (Horizon A); and (ii) the presence of Eocene, Oligocene, and Miocene rocks in the post-Cretaceous stratigraphy in the northern Ceduna Sub-basin (Fig. 2; DR1). A regional 2D seismic profile passing through Potoroo-1 allows us to map the very distinct top Cretaceous reflection into our study area, although overlying, lower-amplitude reflections near the top of the Eocene and Oligocene successions (Fig. 3) are harder to correlate over such a long distance (i.e. c. 300 km) (DR3). However, biostratigraphic data from Potoroo-1 and regional seismic data together provide strong evidence that strata *directly* overlying Cretaceous strata within the study area are almost undoubtedly pre-Quaternary (i.e. older than previous estimates of the onset of Leeuwin Current activity), and more likely Paleocene to Eocene.

Based on seismic-stratigraphic relationships (e.g. onlap, downlap, erosional truncations, changes in seismic facies) we map four key seismic reflections within the study area; the lowermost horizon, A, correlates with the top Cretaceous horizon identified at the location of Potoroo-1, whereas Horizon C defines the top of the middle Eocene volcanoes (Horizons A–D; Figs 1B, 2 and 3). Well-log data from Potoroo-1 and Gnarlyknots-1a indicate the relatively thin (<300 m) Nullarbor Limestone has a fairly constant P-wave velocity of 2100 m s^{-1} (cf. Espurt et al., 2009); this allows us to convert measurements in milliseconds two-way time (ms TWT) to metres (e.g. 100 ms TWT=105 m). Extrusive igneous bodies were identified and mapped using the geometric and geophysical criteria outlined by Totterdell & Schofield (2008), Jackson (2012) and Magee et al. (2013). Our 2D seismic lines are widely spaced relative to the size of the intra-Nullarbor features we describe below, meaning we cannot document their full, three-dimensional external form or internal architecture (cf. Calvin Campbell & Mosher, 2016). However, intra-Nullarbor scours and 'mounded' seismic facies are typically imaged on and can be mapped between, several adjacent seismic lines. In particular, it is clear that the scours are only developed adjacent to and define 'moats' that encircle the volcanic vents (Figs 2 and 4).

Description of intra-Nullarbor seismic facies. We define two main stratal units within the Nullarbor Formation (SU1-2), separated by a major erosional surface (Horizon D; Figs 1B and 4). The base of SU1 is defined by a high-amplitude, laterally-continuous, positive seismic reflection defining the contact between the Pidinga Formation and the Nullarbor Limestone (i.e. Horizon B), or a series of volcanoes (i.e. Horizon C) (Figs 1B and 4). SU1 comprises the lower part of the Nullarbor Limestone and, away from the volcanoes, is typically characterised by low-to-moderate amplitude, parallel-to-sub-parallel, very continuous reflections (Fig. 4). Closer to the volcanoes (i.e. <2 km), a series of gently-dipping (<4°) reflections are developed in SU1, and these locally display bilateral downlap onto the underlying reflections and thus define convex-up, 'mounded' bodies (Figs 4B-D). These inclined reflections, which either dip towards (Fig. 4A) or away (Figs 4C–D) from the volcanoes, typically overlie low-angle (<6°) erosional surfaces, which are up to 2 km wide and display up to 100 m of relief; these surfaces pass laterally into (seismically) conformable surfaces (Fig. 4).

The base of SU2 is locally defined by a major erosion surface along which numerous scours are developed (Horizon D; Figs 1–4). These scours locally define a series of 'moat-like' features that fully or partly encircle 15 of the 57 vents present in the Ceduna Sub-basin (e.g. Fig. 2). The scours have a relief of 10–90 m, extend <3 km from the volcanoes, and their flanks dip 0.1–6.1°, being best-developed around volcanoes that are typically >200 m tall. Some of the scours are asymmetric, consisting of a long, gently dipping outer margin inclined towards the vents and a shorter, more steeply-dipping surface that dips away from the vents (Figs 4B–D). However, our 2D seismic data do not allow us to confidently determine if the scours are consistently asymmetric in one direction, or if they are preferentially developed on one side of the vents (Fig. 2). Two main types of seismic facies fill the scours: (i) high-amplitude, 'mounded' reflections, which have a relief of up to 50 m and a distance of 100–200 m between adjacent mound crests (Fig. 4B); and (ii) low-to-high amplitude, gently-dipping (<2°), moderately discontinuous to laterally-continuous reflections (Fig. 3). The upper part of SU2 is dominated by low-to-high amplitude, flat-lying to gently-dipping (<2°), laterally-continuous reflections (Fig. 4), with erosionally based packages of chaotic reflections being locally developed.

Interpretation of intra-Nullarbor features. Based on their development in a fully marine succession and given that post-Middle Eocene water depths were probably at least several hundred metres (see Jackson, 2012), it is unlikely the intra-Nullarbor scours and mounds formed subaerially. Furthermore, the coeval basin margin, which was likely located several hundred kilometres to the north, was carbonate-dominated and constructional (Fig. 1; see also Feary and James, 1995, 1998), suggesting only limited sediment bypass to deep-water, and that voluminous, strongly erosional gravity currents, such as turbidity currents, were likely not responsible for the formation of the intra-Nullarbor scours and mounds. Although large mounded bodies, typically interpreted as sediment waves, are commonly observed in many deepwater depositional systems, scours of the irregular shape and size to those observed here are not (e.g. Posamentier & Kolla, 2003).

Based on their development in a fully marine succession deposited in several hundreds of metres of water, our preferred interpretation is that the scours formed in response to ocean current-related incision of the seabed (Fig. 5). Such scours are common in modern seas and oceans, typically in association with channel-related contourite drifts (*sensu* Stow et al., 2002). The spatial restriction of Ceduna Sub-basin scours to within c. 3 km of the volcanoes, strongly suggests the volcanic edifices formed syn-incision bathymetric highs that perturbed the velocity structure of the causal ocean currents. We suggest this perturbation increased current turbulence and, most critically, seabed shear stress, driving localised erosion of the seabed immediately adjacent to the volcanoes (Fig. 5) (e.g. O'Reilly et al., 2003; MacLachlan et al., 2008). Submarine scours of broadly similar geometry, dimension, and origin are observed adjacent to igneous rock-cored bathymetric highs in the Pisces Reef system, Irish Sea, UK (Callaway et al., 2009), and in the Capel and Faust basins, offshore eastern Australia (Rollet et al., 2012). Scours are best-developed adjacent to the tallest volcanoes because only these were expressed at the paleoseabed at the onset of the ocean current initiation (see below); shorter volcanoes were buried by this time, thus they lack flanking scours.

We interpret that inclined and mounded reflections developed throughout the Nullarbor Limestone represent dip-oblique and dip-parallel sections, respectively, through contourite drifts (cf. Rebesco and Stow, 2001; Stow et al., 2003; Hohbein et al., 2012; Rebesco et al., 2014). Sedimentary bodies like this are commonly associated with seabed scours, being deposited when bottom current energy is low enough to permit sediment reworking within bedforms (Fig. 5) (e.g. Stow et al., 2002). Like the scours, intra-Nullarbor bedforms are spatially restricted to within a few kilometres of the vents, suggesting they too formed due to volcano-driven perturbations in ocean current velocity and seabed shear stress. In their case, however, an increase in seabed shear stress was only sufficient to rework sediment and not deeply erode the seabed (Fig. 5).

Implications for the paleoceanographic development of the Great Australian Bight. Although the Gnarlyknots-1a borehole penetrates the Nullarbor Formation, no biostratigraphic data were collected; as a result, we cannot constrain the age of intra-Nullarbor scours, associated strata, or indeed, the causal current more tightly than 'middle Eocene-to-Recent'. However, biostratigraphic data from Potoroo-1, correlated into our study area using regional 2D seismic profiles (DR3) does suggest that contourite-bearing strata *directly* overlying Cretaceous strata are very likely pre-Quaternary, and most probably Eocene (Fig. 3; see also DR1 and DR3). No paleobathymetric data (e.g. benthic foraminifera) were collected in Gnarlyknots-1a, meaning we have no direct constraints on water depth variations during post-Cretaceous times, and thus the depth of formation of the contourite drifts remains uncertain (see also discussion in Jackson, 2012). Our relatively widely spaced 2D seismic reflection data also do not allow us to confidently determine if intra-Nullarbor scours are preferentially developed on one, most likely the down-current (i.e. lee) side of the seabed obstruction (i.e. the volcanoes), or if the associated bedforms are best-developed on one, most likely the up-current side of the vents, and display down-current accretion (e.g. Callaway et al., 2009; Rollet et al., 2012). Because of this, we do not know the dominant direction of the causal current.

Notwithstanding these limitations, it is informative to discuss the implications of our study for the Paleogene paleoceanographic evolution of the eastern Great Australian Bight. Using biostratigraphic proxy data from the Bight and Otway basins, McGowran et al. (1997) suggest the initiation of eastwards protrusion of a so-called 'proto-Leeuwin Current' into the Great Australian Bight during the middle Eocene, with further evidence for its presence in the middle Miocene (Fig. 1A; see also Feary and James, 1995, 1998). This interpretation was, however, challenged by Wyroll et al. (2009), who suggest these fauna may simply record locally elevated sea surface temperatures unrelated to the initiation of a plate-scale thermohaline current. We here suggest middle Eocene-to-Recent contourites developed in the Ceduna Sub-basin are associated with Paleogene initiation of an oceanographic current, which we link to the postulated proto-Leeuwin Current, and which operated in broadly similar waters depths (i.e. a few hundred metres) to the present Leeuwin Current (Fig. 5). More specifically, we propose these features record late middle Eocene initiation and subsequent fluctuations in the strength and erosivity of, the current. The major intra-Nullarbor erosion surface (Horizon D), for example, which is best-developed immediately adjacent to the volcanoes, may represent intensification or 'waxing' of the proto-Leeuwin Current (Fig. 5). Despite a lack of age data, we tentatively suggest this erosional event, and related bedforms, may be the stratigraphic expression of the Miocene Climatic Optimum-related event proposed by Feary and James (1995, 1998), during which time anomalously warm waters encroached eastwards into the Great Australian Bight from western Australia (see also Savin et al., 1975; Gourley and Gallagher, 2004). Our interpretation of the timing of onset and dynamics of the Leeuwin Current are at least broadly supported by biostratigraphic data from Potoroo-1 and regional seismic data.

Our study shows that seismic reflection data can image erosional and depositional features that provide a physical stratigraphic record of ancient ocean currents. We demonstrate that by placing these features into a broad chronostratigraphic framework, we can complement rather sparse micro-faunal evidence, and gain important insights into the timing of onset of major ocean currents. Data limitations notwithstanding, our seismic reflection-based approach does, at the very least, provide a clear hypothesis testable with future scientific drilling (e.g. IODP). Seismic reflection data allow erection of a physical, stratigraphic framework and remain an essential part of the paleoceanographer's toolkit. Future work should focus on detailed mapping of seismic reflection datasets from, for example, the western Bight Basin and Otway Basin; this may reveal similar, age-equivalent current-formed stratigraphic features, thus raising the possibility that the proto-Leeuwin Current extended further eastwards and influenced faunal distribution and potentially climate over a wider area than currently assumed.

ACKNOWLEDGEMENTS

Geoscience Australia are thanked for providing seismic and borehole data. We are especially thankful to journal reviewers Sam Johnstone and Brian Romans for providing such insightful, constructive reviews of our paper, and to Andrea Fildani and Gary Hampson for their editorial handling.

REFERENCES

Boldreel, L.O.L., Andersen, M.S., and Kuijpers, A., 1998, Neogene seismic facies and deep-water gateways in the Faeroe Bank area, NE Atlantic: Marine Geology, v. 152, p. 129-140.

Boyle, P.R., Romans, B.W., Tucholke, B.E., Norris, R.D., Swift, S.A., and Sexton, P.F., 2017, Cenozoic North Atlantic deep circulation history recorded in contourite drifts, offshore Newfoundland, Canada: Marine Geology, v. 385, p. 185-203.

Callaway, A., Smyth, J., Brown, C.J., Quinn, R., Service, M., and Long, D., 2009, The impact of scour processes on a smothered reef system in the Irish Sea: Estuarine, Coastal and Shelf Science, v. 84, p. 409–418.

Campbell, D.C., Mosher, D.C., 2015. Geophysical evidence for widespread Cenozoic bottom current activity from the continental margin of Nova Scotia, Canada: Marine Geology, v. 378, p. 237-260.

Caputi, N., Chubb, C.F., and Pearce, A., 2001, Environmental effects on recruitment of the western rock lobster, Panulirus Cygnus: Marine and Freshwater Research, v. 52, p. 1167-1175.

Cann, J.H., and Clarke, J.A.D., 1993, The significance of *Marginopora vertebralis* Foraminifera in surficial sediments at Esperance, Western Australia and in last interglacial sediments in northern Spencer Gulf: Marine Geology, v. 111, p. 171–187.

Cresswell, G., and Goldring, T., 1980, Observations of a south-flowing current in the southeastern Indian Ocean: Deep Sea Research Part 1: Oceanographic Research Papers, v. 27, p. 449-466.

Cresswell, G.R., and Domingues, C.M., 2009, The Leeuwin Current south of Western Australia: Journal of the Royal Society of Western Australia, 92: 83–100, 2009

Davies, R.J., Cartwright, J.A., Pike, J., and Line, C., 2001, Early Oligocene initiation of North Atlantic deep water formation: Nature, v. 410, p. 917-920.

Due, L., van Aken, H.M., Boldreel, L.O., and Kuijpers, A., 2006, Seismic and oceanographic evidence of present-day bottom-water dynamics in the Lousy Bank-Hatton Bank area, NE Atlantic. Deep Sea Research Part 1: Oceanographic Research Papers, v. 53, p. 1729-1741.

Espurt, N., Callot, J-P., Totterdell, J., Struckmeyer, H., and Vially, R., 2009, Interaction between continental breakup dynamics and large-scale delta system evolution: insights from the Cretaceous Ceduna delta system, Bight Basin, southern Australian margin: Tectonics, v. 28, TC6002.

Faugères, J.C., Stow, D.A.V, Imbert, P., and Viana, A., 1999, Seismic features diagnostic of contourite drifts. Marine Geology, v. 162, p. 1-38.

Feary, D.A., and James, N.P., 1995, Cenozoic biogenic mounds and buried Miocene (?) barrier reef on a predominantly cool-water carbonate continental margin, Eucla Basin, western Great Australian Bight: Geology, v. 23, p. 427-430.

Feary, D.A., and James, N.P., 1998, Seismic Stratigraphy and Geological Evolution of the Cenozoic, Cool-Water Eucla Platform, Great Australian Bight: AAPG Bulletin, v. 82, p. 792-816.

Feng, M., Waite, A., and Thompson, P., 2009, Climate variability and ocean production in the Leeuwin Current system off the west coast of Western Australia: Journal of the Royal Society of Western Australia, v. 92, p. 67-81.

Gourley, T.L., and Gallagher, S.J., 2004, Foraminiferal biofacies of the Miocene warm to cool climatic transition in the Port Phillip Basin, southeastern Australia: Journal of Foraminiferal Research, v. 34, p. 294-307.

Henderson, G.M., 2002, New oceanic proxies for paleoclimate, Earth and Planetary Science Letters, v. 203, 1-13.

Hohbein, M., Sexton, P.F., and Cartwright, J.A., 2012, Onset of North Atlantic Deep Water production coincident with inception of the Cenozoic global cooling trend: Geology, v. 40, p. 255-258.

Huber, M., Brinkhuis, H., Stickley, C.E., Döös, K., Sluijs, A., Warnaar, J., Schellenberg, S.A., and Williams, G.L., 2004, Eocene circulation of the Southern Ocean: Was Antarctica kept warm by subtropical waters? Paleoceanography, v. 19, PA4026.

IPCC, 2007, Climate Change 2007: The physical science basis. Contribution of Working Group I to the Fourth Assessment Report of the Intergovernmental Panel on Climate Change (eds. Solomon, S., Qin, D., Manning, M., Chen, Z., Marquis, M., Averyt, K.B., Tignor, M., and Miller, H.L). Cambridge University Press, Cambridge.

Jackson, C.A-L., 2012, Seismic reflection imaging and controls on the preservation of ancient sill-fed magmatic vents: Journal of the Geological Society, v. 169, p. 503-506.

Janocko, M., Nemec, W., Henriksen, S. and Warchoł, M., 2013, The diversity of deep-water sinuous channel belts and slope valley-fill complexes. Marine and Petroleum Geology, 41, p.7-34.

MacLachlan, S.E., Elliott, G.M., and Parsons, L.M., 2008, Investigations of the bottom current sculpted margin of the Hatton Bank, NE Atlantic: Marine Geology, v. 253, p. 170-184.

Magee, C., Hunt-Stewart, E., and Jackson, C.A-L., 2013, Volcano growth mechanisms and the role of sub-volcanic intrusions: Insights from 2D seismic reflection data: Earth and Planetary Science Letters, 373, p. 41-53.

McGowran, B., Qianyu, L., Cann, J., Padley, D., McKirdy, D.M., and Shafik, S., 1997, Biogeographic impact of the Leeuwin Current in southern Australia since the late Middle Eocene: Palaeogeography, Palaeoclimatology, Palaeoecology, v. 136, p. 19-40.

Müller-Michaelis, A., Uenzelmann-Neben, G., and Stein, R., 2013, A revised Early Miocene age for the instigation of the Eirik Drift, offshore southern Greenland: Evidence from high-resolution seismic reflection data: Marine Geology, v. 340, p. 1-15.

Posamentier, H.W. and Kolla, V., 2003, Seismic geomorphology and stratigraphy of depositional elements in deep-water settings. Journal of sedimentary research, 73, p. 367-388.

O'Reilly, B., Readman, P.W., Shannon, P.M., and Jacob, A.W.B., 2003, A model for the development of a carbonate mound population in the Rockall Trough based on deep-towed sidescan sonar data: Marine Geology, v. 198, p. 55-66.

Rahmstorf, S., 2003, The current climate: Nature, v. 421, p. 699.

Rebesco, M., and Stow, D., 2001, Seismic expression of contourites and related deposits: a preface: Marine Geophysical Researches, v. 22, p. 303–308.

Rebesco, M., Hernández-Molina, F.J., Van Rooij, D., Wåhlin, A., 2014. Contourites and associated sediments controlled by deep-water circulation processes: state-of-the-art and future considerations: Marine Geology, 352, p.111-154.

Rollet, N., McGiveron, S., Hashimoto, T., Hackney, R., Petkovic, P., Higgins, K., Grosjean, E., Logan, G.A., 2012, Seafloor features and fluid migration in the Capel and Faust basins, offshore eastern Australia: Marine and Petroleum Geology, v. 35, p. 269–291.

Savin, S.M., Douglas, R.G., and Stehli, F.G., 1975, Tertiary marine paleotemperatures: Geological Society of American Bulletin, v. 86, p. 1499–1510.

Schofield, A., and Totterdell, J., 2008, Distribution, timing and origin of magmatism in the Bight and Eucla basins: Australian Government Report, 2008/24.

Shafik, S., 1983, Calcareous nannofossil biostratigraphy: an assessment of foraminiferal and sedimentation events in the Eocene of the Otway Basin, southeastern Australia: Journal of Australian Geology and Geophysics, v. 8, p. 1-17.

Shafik, S., 1990, The Maastrichtian and early Tertiary record of the Great Australian Bight Basin and its onshore equivalents on the Australian southern margin: a nannofossil study: Bureau of Mineral Resources Journal of Australian Geology and Geophysics, v. 11, p. 473-497.

Stickley, C.E., Brinhuis, H., Schellenberg, S.A., Sluijs, A., Röhl, U., Fuller, M,. Grauert, M., Huber, M., Warnaar, J., and Williams, G.L., 2004, Timing and deepening of the Tasmanian Gateway. Paleoceanography, v. 19: PA4027.

Stow, D.A.V., Faugères, J.C., Howe, J.A., Pudsey, C.J., and Viana, A.R., 2003, Bottom currents, contourites and deep-sea sediment drifts: Current state-of-the-art, in Stow, D.A.V., et al., eds., Deep-water contourite systems: Modern drifts and ancient series, seismic and sedimentary characteristics: The Geological Society of London Memoir, v. 22, p. 73–84.

Tucholke, B.E., 1979, Relationships between acoustic stratigraphy and lithostratigraphy in the western North Atlantic Basin, in: Tucholke, B.E., Vogt, P.R. (Eds.), Initial Reports of the Deep Sea Drilling Project, Vol. 43. U.S. Government Printing Office, Washington, D.C., pp. 827-846.

Tucholke, B.E., and Mountain, G.S., 1979, Seismic stratigraphy, lithostratigraphy and paleosedimentation patterns in the North American Basin, in: Talwani, M., Hay, W., Ryan, W.B.F. (Eds.), Deep Drilling in the Atlantic Ocean: Continental Margins and Paleoenvironment, Maurice Ewing Series 3. American Geophysical Union, Washington, D.C., pp. 58-86.

von Blanckenburg, F., 1999, Palaeoceonography: tracing past ocean circulation?: Science, v. 286, p. 1862-1863.

Wunsch, C., 2002, What is the thermohaline circulation?: Nature, v. 298, p. 1179-1181.

Wyrwoll, K-H., Greenstein, B.J., Kendrick, G.W., and Chen, G.S., 2009, The palaeoceanography of the Leeuwin Current: implications for a future world. Journal of the Royal Society of Western Australia, v. 92, p. 37–51.

FIGURE CAPTIONS

Fig 1. (A) Map illustrating the geographical setting of the study area. The area covered by 2D seismic reflection data is outlined by a solid black line. Inset shows the key modern oceanographic currents developed along the western and southern Australian margin. LC=Leeuwin Current; ACC=Antarctic Circumpolar Current; WAC=West Australia Current; FC=Flinders Current. OB=Otway Basin. Modified from Jackson (2012); oceanographic currents from Bilj et al. (2013). Grey dashed lines indicate boundaries between sub-basins forming part of the Great Australian Bight. (B) Simplified stratigraphic column based on data from boreholes Gnarlyknots-1A and Potoroo-1. Key seismic horizons (A–D) and seismic units (SU1-2) are indicated. The stratigraphic occurrence of intrusion and extrusive components of the Bight Basin Igneous Complex (BBIC) are shown. Modified from Jackson (2012).

Fig. 2. Time-structure map of the Horizon B (base Nullarbor Limestone) clipped where it intersects Horizon C (top volcanic vents); this illustrates the distribution of volcano summits (labelled ‘v’ and encircled by a solid white line) that rise above Horizon D, and intra-SU2 scours (labelled ‘s’). d=drifts. (A) and (B) are from the southern and northern parts of the study area respectively. See Figure 1A for location of map. Light grey lines indicate seismic reflection profiles. Note that the geometries of the Horizons C and D are poorly constrained away from the 2D seismic reflection profiles.

Fig. 3. Interpreted seismic profile through the Potoroo-1 borehole, showing the age constraints on the key, regionally mappable seismic horizon ‘A’ (top Upper Cretaceous) (see

also DR1 and DR2) and the development of contour current-related features (d=drifts; s=scours) in the Paleocene-Eocene sequence. See Fig. 1A and DR2 for location of Potoroo-1.

Fig. 4. (A)–(D) Interpreted seismic profiles illustrating the geometry, scale and relationship between extrusive volcanic features of the Bight Basin Igneous Complexes and intra-Nullabor Limestone contourites (i.e. scours and bedforms). Locations of the seismic lines are shown in Figure 2. Note the vertical scale is provided in ms TWT and metres, based on an intra-Nullarbor interval velocity of 2100 m s^{-1}. Uninterpreted versions of sections are available in DRI1.

Fig. 5. (A–C) Schematic diagrams illustrating the evolution of intra-Nullarbor Limestone contourites in the Great Australia Bight. The vertical dashed line in the 'current strength' column indicates the threshold for sediment erosion/non-deposition; these conditions occur at the onset of T2.

Data Repository Item (DR1). Biostratigraphic and age data from Potoroo-1 (data: http://dbforms.ga.gov.au/www/npm.well.summary_report?pEno=14937&pName=Potoroo%20%201&pTimescale=A&pTotalDepth=987.75&pDepthMax=987.75&pDepthMin=0&pPeriod=&pStage=&pAgeMax=65.5&pAgeMin=0&pAgeTop=0&pAgeBase=135&pTotalAge=135&pPrinterV=Yes). Data accessed on December 5th 2018. Well location: Lat -33 23' 13.571" S, Long 130 46' 6.899" E. Ages are calibrated to International Chronostratigraphic Chart v2018/08 of the International Stratigraphic Commission (ISC) (http://www.stratigraphy.org/index.php/ics-chart-timescale).

Data Repository Item (DR2). Uninterpreted version of the seismic profile presented in Fig. 3.

Data Repository Item (DR3). Regional seismic profile between Potoroo-1, Gnarlyknots-1, and our general area of study (see Figs. 3 and 4). Note the persistence of the high-amplitude, top Cretaceous seismic reflection and the seismic-scale continuity of the overlying Eocene, Oligocene, and Miocene rocks (see Fig. 3 and DR1). Location shown in Fig. 1A.

Data Repository Item (DR4). Uninterpreted versions of the seismic profiles presented in Fig. 4.

Fig. 1

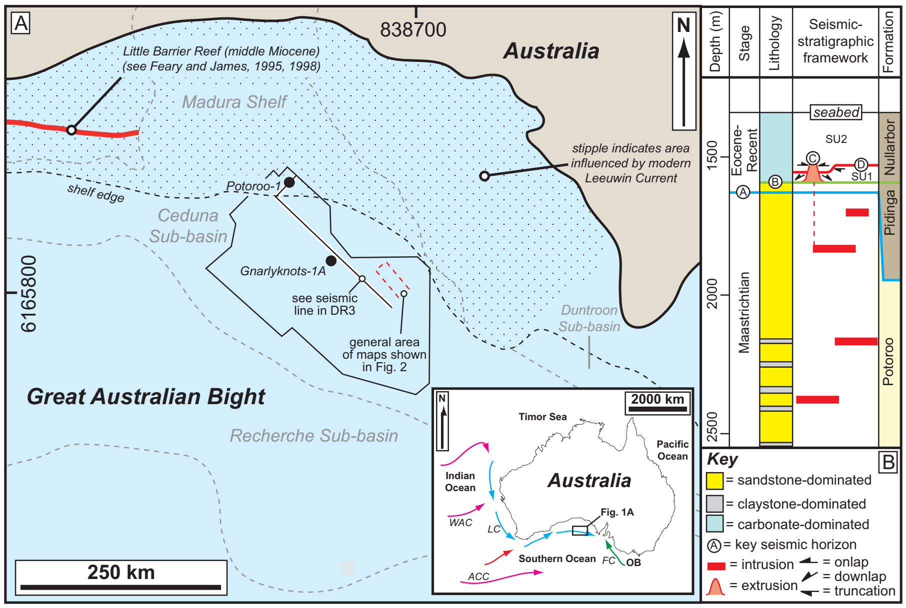

A
838700
Australia
N
Little Barrier Reef (middle Miocene)
(see Feary and James, 1995, 1998)
Madura Shelf
stipple indicates area
influenced by modern
Leeuwin Current
shelf edge
Potoroo-1
Ceduna
Sub-basin
Gnarlyknots-1A
see seismic
line in DR3
general area
of maps shown
in Fig. 2
6165800
Duntroon
Sub-basin
Great Australian Bight
Recherche Sub-basin
250 km
2000 km
Timor Sea
Pacific
Ocean
Indian
Ocean
Australia
WAC
LC
Fig. 1A
Southern Ocean
FC
OB
ACC
Depth (m)
Stage
Lithology
Seismic-
stratigraphic
framework
Formation
seabed
SU2
SU1
Eocene-
Recent
Maastrichtian
1500
2000
2500
Nullarbor
Pidinga
Potoroo
B
Key
= sandstone-dominated
= claystone-dominated
= carbonate-dominated
= key seismic horizon
= intrusion
= extrusion
= onlap
= downlap
= truncation

Fig. 2

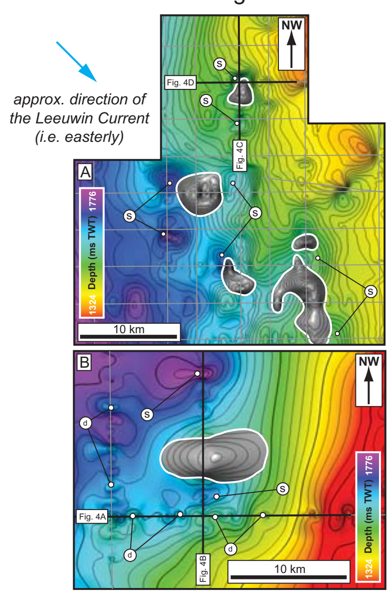
approx. direction of
the Leeuwin Current
(i.e. easterly)
A
NW
Fig. 4D
Fig. 4C
1324 Depth (ms TWT) 1776
10 km
S
B
NW
Fig. 4A
Fig. 4B
d
1324 Depth (ms TWT) 1776
10 km

Fig. 3

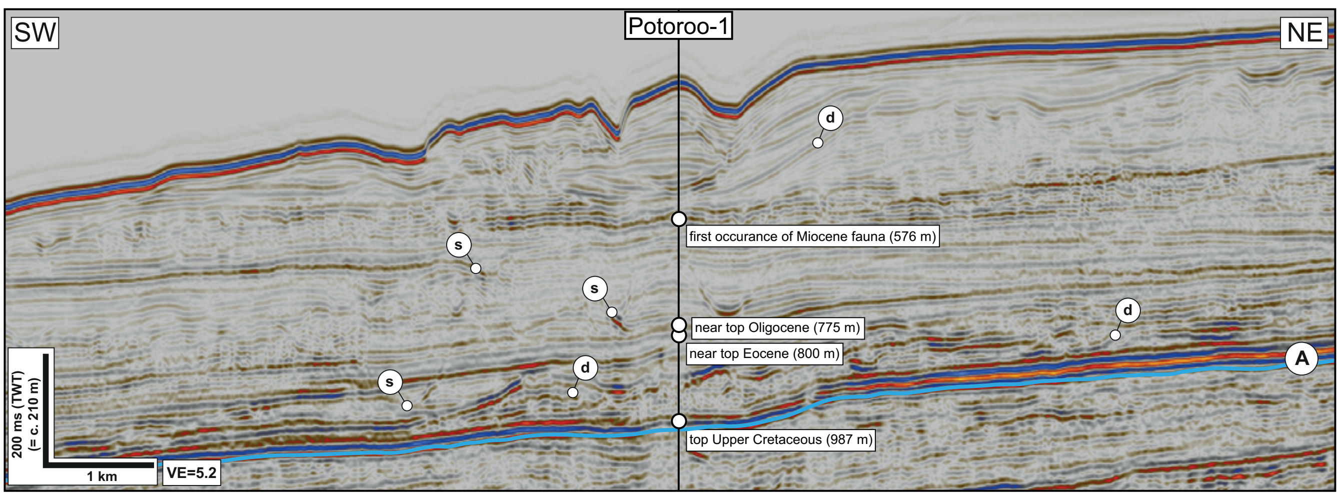

SW
Potoroo-1
NE
d
first occurance of Miocene fauna (576 m)
s
s
near top Oligocene (775 m)
near top Eocene (800 m)
d
A
s
d
200 ms (TWT)
(= c. 210 m)
top Upper Cretaceous (987 m)
1 km
VE=5.2

Fig. 4

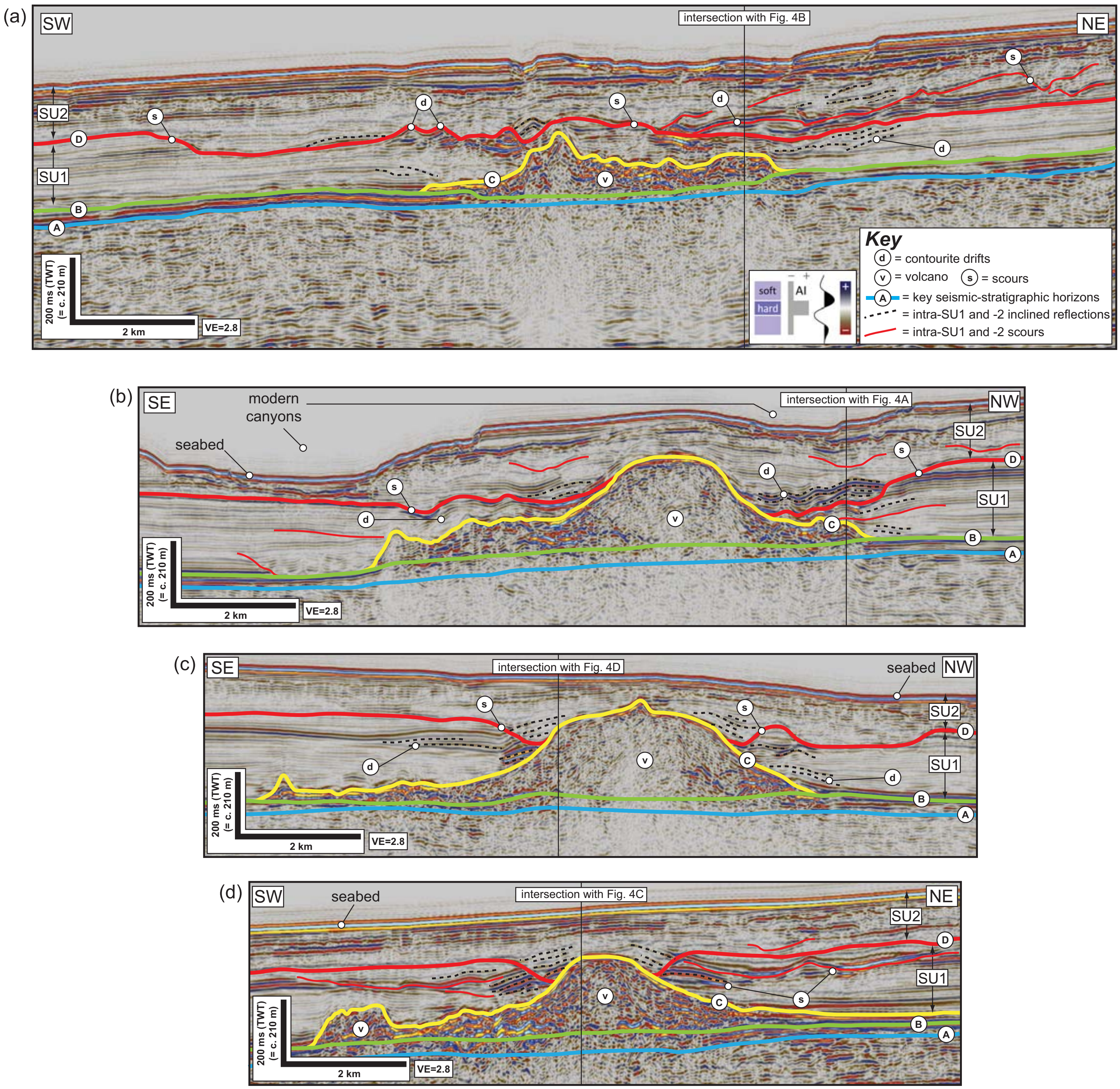

(a)
SW
intersection with Fig. 4B
NE
SU2
SU1
Key
d = contourite drifts
v = volcano
s = scours
A = key seismic-stratigraphic horizons
= intra-SU1 and -2 inclined reflections
= intra-SU1 and -2 scours
soft
hard
AI
200 ms (TWT) (= c. 210 m)
2 km
VE=2.8
(b)
SE
modern canyons
seabed
intersection with Fig. 4A
NW
SU2
SU1
200 ms (TWT) (= c. 210 m)
2 km
VE=2.8
(c)
SE
intersection with Fig. 4D
seabed
NW
SU2
SU1
200 ms (TWT) (= c. 210 m)
2 km
VE=2.8
(d)
SW
seabed
intersection with Fig. 4C
NE
SU2
SU1
200 ms (TWT) (= c. 210 m)
2 km
VE=2.8

Fig. 5

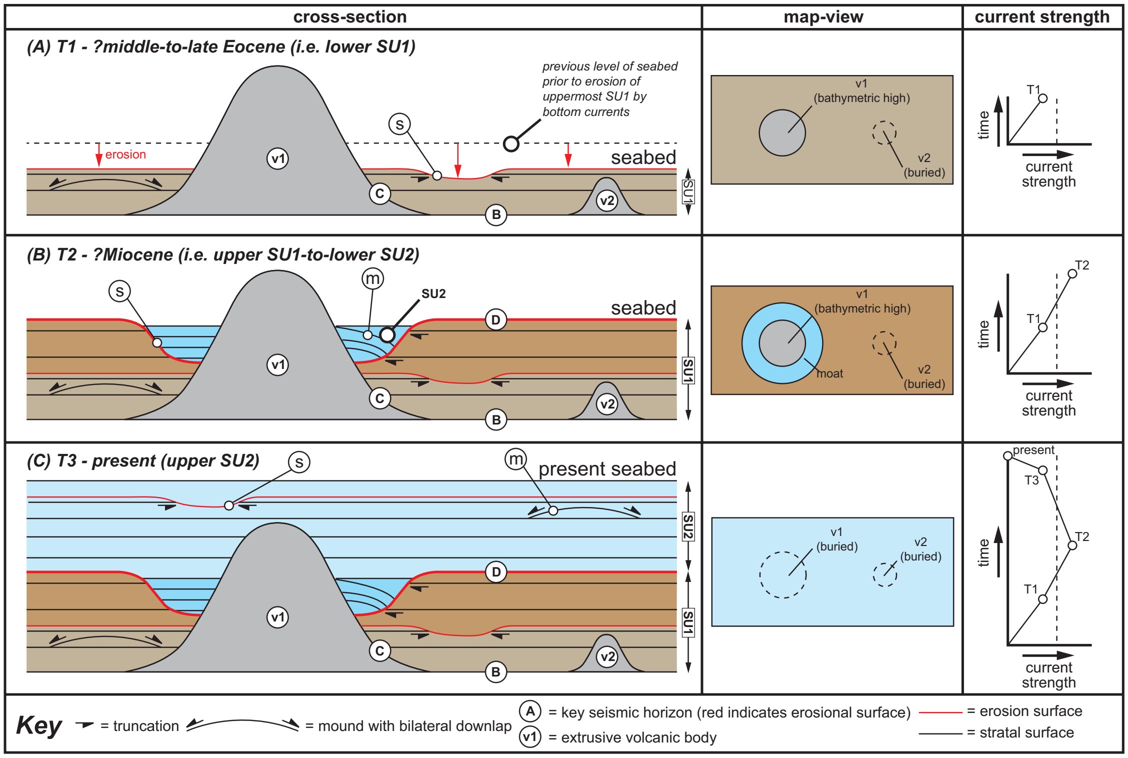

cross-section
map-view
current strength
(A) T1 - ?middle-to-late Eocene (i.e. lower SU1)
previous level of seabed prior to erosion of uppermost SU1 by bottom currents
erosion
seabed
s
v1
C
B
v2
SU1
v1 (bathymetric high)
v2 (buried)
T1
time
current strength
(B) T2 - ?Miocene (i.e. upper SU1-to-lower SU2)
m
SU2
D
moat
T2
(C) T3 - present (upper SU2)
present seabed
v1 (buried)
v2 (buried)
present
T3
Key
= truncation
= mound with bilateral downlap
A = key seismic horizon (red indicates erosional surface)
v1 = extrusive volcanic body
= erosion surface
= stratal surface